Analyses of ZPPR-21 Benchmarks with ENDF/B-V and -VII Data

Sang Ji Kim[a*], Changho Lee[b], Won Sik Yang[b], Yeong-il Kim[a]
[a]*Korea Atomic Energy Research Institute, 1045 Daedeog-Daero, Yuseong-gu, 305-353 Daejeon, Korea*
[b]*Argonne National Laboratory, 9700 S. Cass Avenue, Argonne, Il 60439, U.S.A.*
[*]*Corresponding author: sjkim3@kaeri.re.kr*

1. Introduction

The six benchmark problems for the ZPPR-21 critical experiments phases A through F were analyzed using the ENDF/B-V.2 and ENDF/B-VII.0 data. For reference calculations, Monte Carlo simulations were performed using the VIM code with the continuous energy cross sections.

For deterministic calculations, composition and region dependent multi-group cross sections were generated using the ETOE-2/MC2-2/SDX code system and core calculations were performed with the TWODANT discrete ordinate transport code.

The purpose of this effort is to validate the neutronics design tools and nuclear data for fast reactor analyses against previous critical experiments.

2. Description of ZPPR-21 Critical Benchmarks

The ZPPR Assembly 21 consists of a series of six criticality benchmark cores built in the ZPPR facility to provide data for validating criticality calculations for systems likely arising in the Integral Fast Reactor (IFR) fuel processing operations. The assemblies were graphite reflected, and different mixtures of plutonium and uranium were used in mock-up Pu-U-Zr fuel. The first configuration, ZPPR-21A [1], was built with only plutonium fuel to take advantage of the inherent neutron source of Pu-240. Then, enriched uranium was progressively substituted for plutonium in Phases B through E [2]. The final configuration, ZPPR-21F [3], had an all-uranium fuel loading.

The benchmark model geometry for ZPPR-21 Phase A is depicted in Fig. 1. Except for the thicknesses of the radial graphite reflector and voided drawers, benchmark geometries remain the same throughout all the phases of ZPPR-21.

3. Methods and Results

3.1 Reference Monte Carlo Calculations

Reference solutions were obtained from VIM Monte Carlo calculations with the cross section libraries based on ENDF/B-V.2 and ENDF/B-VII.0 data. Thirty million histories were used per assembly. For independent check of the ENDF/B-VII.0 library of VIM [4], MCNP4C calculations were also performed. The k_{eff} values are summarized in Table I. The cited VIM k_{eff} values were obtained from the combined estimator of analog and track length estimators. For all six core configurations,

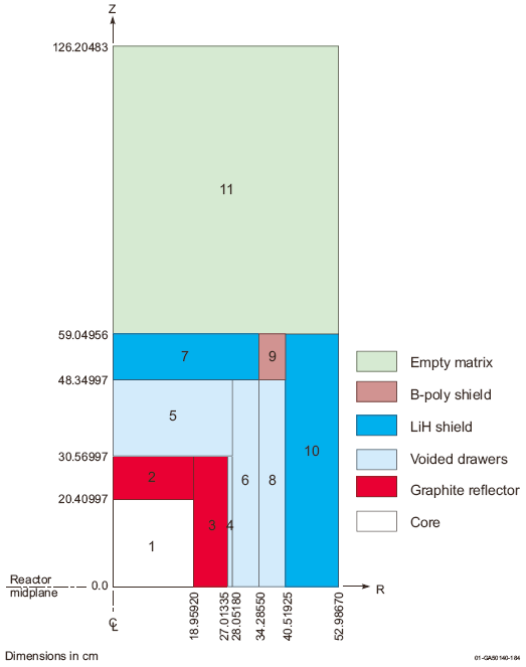

Fig. 1. Benchmark model geometry for ZPPR-21A

the estimated standard deviation of the Monte Carlo simulation is less than or equal to 20 pcm Δk. With such a small standard deviation, the isotopic reaction rate edited from the VIM calculations was able to be used for a detailed comparison with the TWODANT results.

Table I: k_{eff} Results for ZPPR-21 phases A through F

Config	Benchmark [a)]	ENDF/B-V.2	ENDF/B-VII.0	
		VIM [b)]	VIM [c)]	MCNP4C [d)]
A	0.9974	1.00000	0.99910	0.99869
B	0.9897	0.99251	0.99325	0.99293
C	0.9998	0.99788	0.99945	0.99923
D	1.0018	0.99971	1.00312	1.00345
E	1.0012	1.00002	1.00494	1.00485
F	0.9998	1.00053	1.00648	1.00612

* standard deviations ≤ a) 0.0026, b) 0.00017, c) 0.00015, d) 0.00020

3.2 Deterministic Core Calculations

For each configuration, region-wise cross sections were generated using the MC^2-2 code [5]. The MC^2-2 calculations were performed with the consistent P_1 or B_1 approximation, and anisotropic scattering cross sections were generated for Legendre orders up to five. A critical buckling search was conducted for the active core region. For non-fueled regions, fixed source calculations

were performed with an estimated leakage spectrum from adjacent regions.

Fine mesh RZ geometry models were established for TWODANT calculations with 1 cm radial and axial mesh intervals which were found fine enough to yield converged solutions. Using the 230-group, fine-mesh models and ENDF/B-V.2 data, sensitivity studies were carried out to determine the level of modeling details required for converged deterministic solutions, in terms of energy group, spatial mesh size, angular approximation, and anisotropic scattering order. Core multiplication factor, leakage fraction, and isotopic principal cross sections were also monitored. It was observed that a higher order anisotropic scattering approximation is required to accurately represent the large leakage fraction.

Table II shows the TWODANT core k_{eff} results compared with benchmark values and VIM results. The TWODANT results were obtained from $S_{24}P_5$ calculations. Using ENDF/B-V.2 data, the TWODANT k_{eff} values are well within the 1-sigma measurement uncertainty, except for configurations B and C for which the deviation is between the 1 and 2-sigma uncertainties. The mean and 1-sigma standard deviation of the differences between the TWODANT and benchmark k_{eff} values for the six configurations are -20 and 230 pcm, respectively. As can be seen, TWODANT results are very consistent with VIM results. For ENDF/B-VII.0 data, TWODANT results agreed reasonably with VIM results within 270 pcm, but the VIM Monte Carlo results overestimated k_{eff} in most configurations and significantly for the configuration F, compared to the benchmark results

Along with the verification results against VIM calculations discussed previously, these results for the ZPPR-21 critical assemblies show that (1) the accuracy of the MC^2-2/TWODANT system for core k_{eff} estimation is comparable to the VIM Monte Carlo code and (2) the multigroup cross sections generated with MC^2-2 accurately reproduce the isotopic reaction rates of VIM calculations.

4. Conclusions

For all six ZPPR-21 configurations, the core multiplication factor determined with a 230-group TWODANT calculation agreed with the VIM Monte Carlo solution within 0.20 %Δk for ENDF/B-V.2 and 0.27 %Δk for ENDF/B-VII.0. There was no indication of any systematic bias. Analyses of principal cross sections from ENDF/B-V.2 data indicated that the quality of those cross sections generated with the MC^2-2 code was comparable to that of VIM cross sections. The overall reactivity effect due to the errors in the 230-group principal cross sections was estimated to be less than 0.05 %Δk. The statistics of the differences between calculated values and specified benchmark experimental values showed similar bias (from -0.28 %Δk to 0.33 %Δk) for MC^2-2/TWODANT and VIM. This result indicates that the criticality prediction accuracy of MC^2-2/TWODANT is comparable to VIM.

Acknowledgement

This study was supported by Ministry of Education, Science Technology (MEST) in Korea through its National Nuclear Technology Program.

REFERENCES

[1] R. M. Lell, R. W. Schaefer, R. D. McKnight, and A. Mohamed, "ZPPR-21 Phase A: A Cylindrical Assembly of Pu Metal Reflected by Graphite," PU-MET-FAST-033, NEA/NSC/DOC(95)03 (2005).

[2] R. D. McKnight, R. M. Lell, R. W. Schaefer, and A. Mohamed, "ZPPR-21 Phases B through E: Cylindrical Assemblies of Mixed Fissile Pu and U Metal Reflected by Graphite," MIX-MET-FAST-011, NEA/NSC/DOC(95) 03 (2005).

[3] R. W. Schaefer, R. D. McKnight, R. M. Lell, and A. Mohamed, "ZPPR-21 Phase F: A Cylindrical Assembly of U Metal Reflected by Graphite," HEU-MET-FAST-061, NEA/NSC/DOC(95)03 (2005).

[4] R. N. Blomquist, "VIM Continuous Energy Monte Carlo Transport Code," Proc. Intl. Conf. on Mathematics, Computations, Reactor Physics and Environmental Analysis, Portland, OR, April 30-May 4 (1995).

[5] H. Henryson II, B. J. Toppel, and C. G. Stenberg, "MC^2-2: A Code to Calculate Fast Neutron Spectra and Multigroup Cross Sections," ANL-8144, Argonne National Laboratory (1976).

TABLE II: Comparison of TWODANT k_{eff} results with benchmark values (Δk, pcm)

Configuration	ENDF/B-V.2			ENDF/B-VII.0		
	VIM – Benchmark	TWODANT-Benchmark	VIM – TWODANT	VIM – Benchmark	TWODANT-Benchmark	VIM – TWODANT
A	260 ±280	130 ±260	-127 ±17	170 ±280	20 ±260	-154 ±15
B	280 ±250	320 ±230	42 ±16	360 ±250	430 ±230	76 ±15
C	-190 ±250	-280 ±230	-90 ±16	-40 ±240	-90 ±230	-51 ±14
D	-210 ±260	-140 ±240	71 ±15	130 ±250	410 ±240	274 ±14
E	-120 ±260	-110 ±240	6 ±17	370 ±250	540 ±240	161 ±14
F	70 ±270	-130 ±250	-201 ±15	670 ±260	660 ±250	-5 ±14